doi:10.1038/nature09736

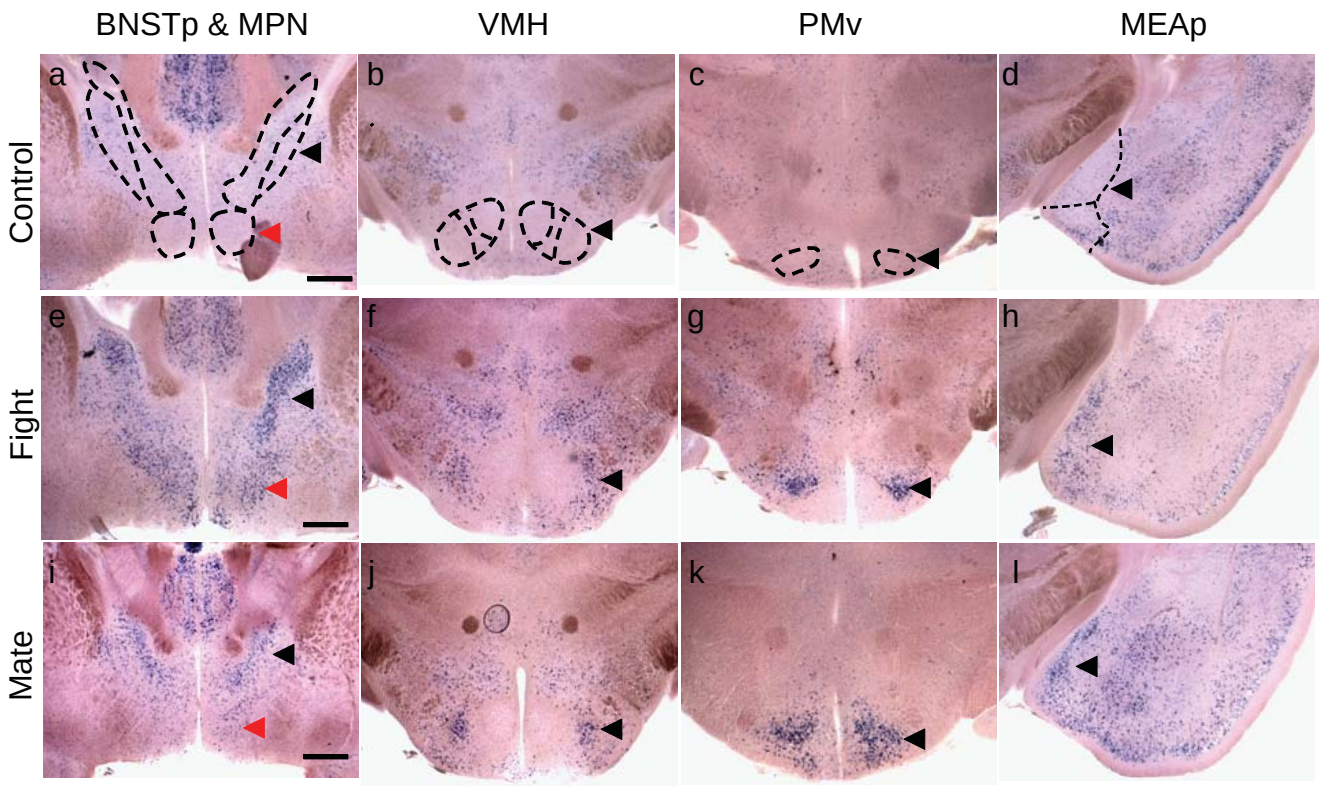

Supplementary Figure S1. Fos activation patterns after male sexual and aggressive behaviors.

Non-isotopic in situ hybridization for *c-fos* mRNA. Dashed lines circumscribe structures of interest. Arrowheads indicate areas of *c-fos* induction. BNSTp: Bed nucleus of the stria terminalis, posterior part (**a**, **e, i,** black arrowheads); MPN: Medial preoptic nucleus (**a, e, i,** red arrowheads); VMHvl: Ventrolateral portion of ventromedial hypothalamic nucleus; PMv: Ventral premammilary nucleus; MEAp: Medial amygdala posterior part.

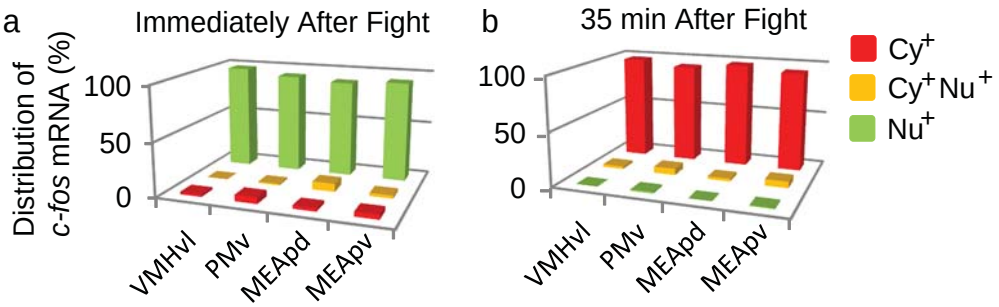

Supplementary Figure S2. Distribution of Fos localization immediately and 35min after fighting.

Percentage of total *c-fos*$^{+}$ cells exhibiting exclusively cytoplasmic (Cy^{+}), nuclear (Nu^{+}) or cytoplasmic + nuclear ($Cy^{+}Nu^{+}$) *c-fos* transcripts immediately after 5min fighting (**a**) or 35min after 5min fighting (**b**).

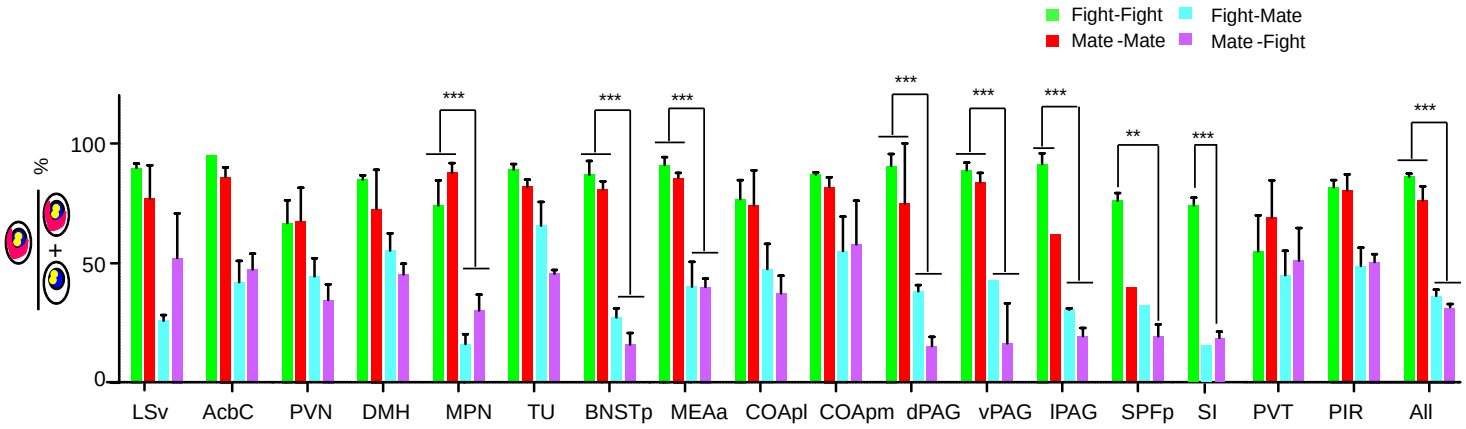

Supplementary Figure S3. Overlap between mating-and fighting-related fos+ populations in various regions

In the MPN, BNSTp, MEAa, dPAG, vPAG, lPAG, SPFp and SI, if the animal experiences the same behavior twice ("Mate-Mate" or "Fight-Fight"), most cells activated during the second behavior are also activated during the first behavior. In contrast, if the animal experiences two different behaviors ("Mate-Fight" or "Fight-Mate"), a significantly lower percentage of cells which are activated during the second behavior was also activated during the first behavior (One-way ANOVA). In other regions including LSv, AcbC, PVN, DMH, TU, COApl, COApm, PVN and PIR, there was no significant difference in the level of overlap between animals experiencing the same or different behaviors. Green bar: Fight-Fight; Red bar: Mate-Mate; Blue bar: Fight - Mate; Magenta bar: Mate – Fight. MPN: Medial preoptic nucleus. MEAa: Medial amygdala, anterior. dPAG: Periaqueductal gray, dorsal part. vPAG: Periaqueductal gray, ventral part. lPAG: Periaqueductal gray, lateral part. SPFp: Parvocellular subparafascicular nucleus. LSv: Lateral septum ventral part. AcbC: Accumbens nuclues, core. PVN: Paraventricular nucleus. DMH: Dorsomedial hypothalamic nucleus. COApl: Cortical amygdalar area, posterior part, lateral zone. COApm: Cortical amygdalar area, posterior part, medial zone. PIR: Piriform cortex. TU: Tuberal nucleus.

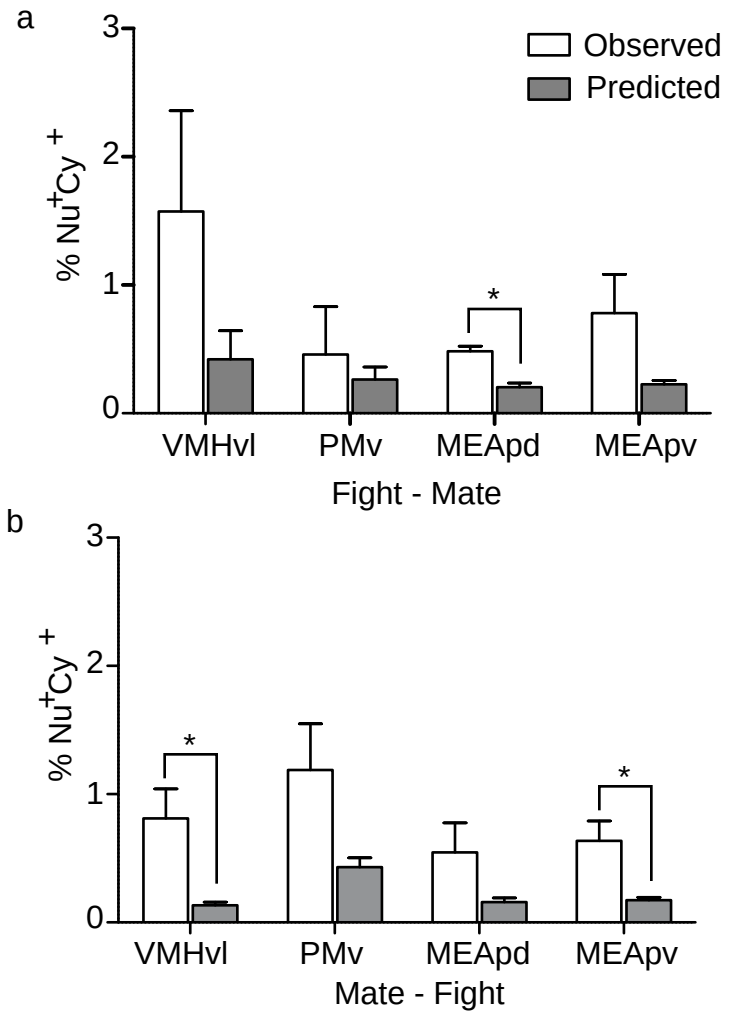

Supplementary Figure S4. Comparison of predicted and observed overlap between mating and fighting subpopulations

After fight-mate (**a**) or fight-mate (**b**), the observed overlap between the populations expressing *c-fos* transcripts after successive episodes of mating and fighting (% nuclear + cytoplasmic *c-fos*$^+$; white bars) was significantly higher in some regions (* $p < 0.05$, t-test) than predicted value (gray bars). The predicted value was calculated as: (% nuclear *c-fos*$^+$ x % cytoplasmic *c-fos*$^+$)/Total No. of neurons x100%.

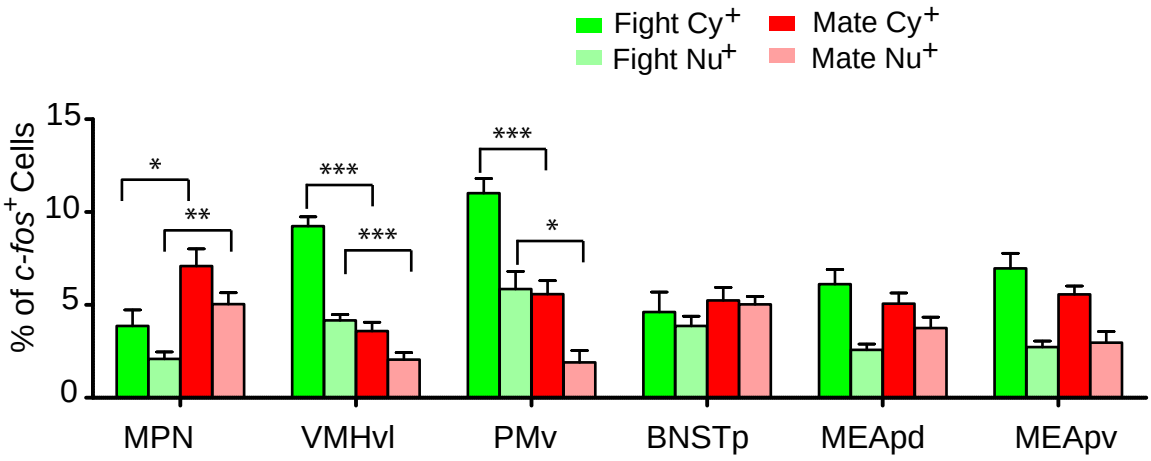

Supplementary Figure S5. Percentage of mating or fighting induced *c-fos*$^+$ cells in various regions

Histograms show the percentage of *c-fos*$^+$ cells among all the neurons after fighting or mating. Green bars: 35 min after fighting; cytoplasmic *c-fos*; Red bars: 35 min after mating; cytoplasmic *c-fos*; Light green bars: Immediately after fighting; nuclear *c-fos*; Light red bars: Immediately after mating; nuclear *c-fos*. *$p < 0.05$, ** $p < 0.01$, *** $p < 0.001$.

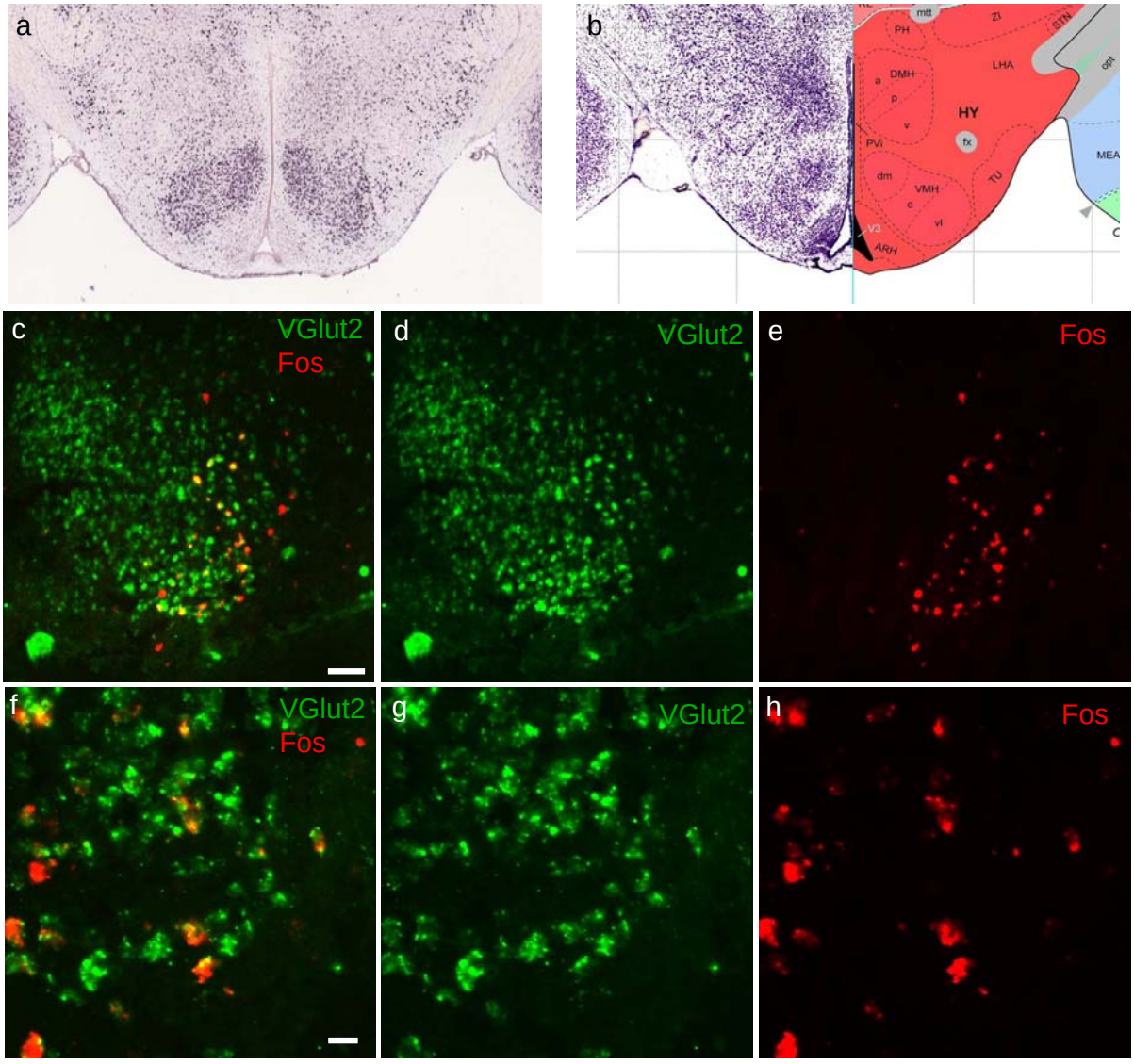

Supplementary Figure S6: Overlap between aggression induced *fos* and Vesicular Glutamate Transporter 2 (*vglut2*) in the VMHvl

a, Colorimetric *in situ* hybridization for *Vglut2* mRNA (Allan Brain Atlas; www.brain-map.org). **b**, The Allen Reference Atlas and Nissl staining for (**a**). **c-e** and **f-h**, 10x and 40x confocal images of double in situ hybridization for *vglut2* (green) and aggression induced c-*fos* mRNAs (red). Scale bars in (**c-e**): 50µm. Scale bars in (**f-h**): 10µm.

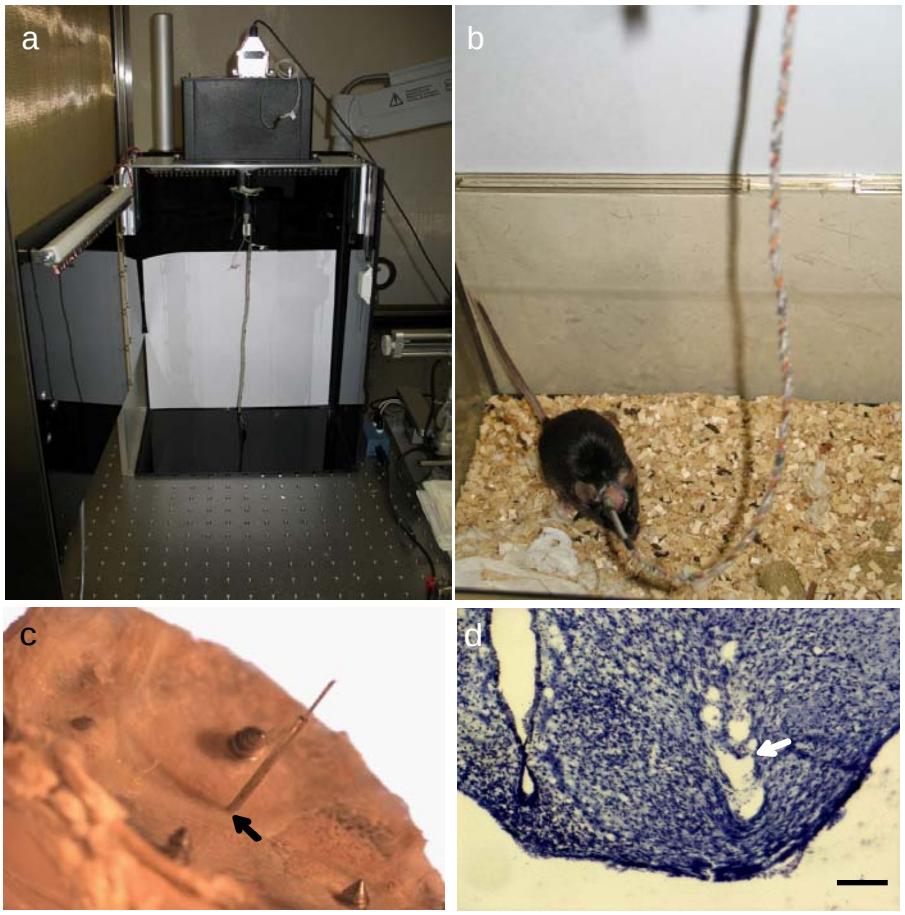

Supplementary Figure S7. Histological analysis of chronic recording sites

a, Custom designed chronic recording chamber featuring infrared LED illumination, commutator and water delivery port from the side. The home cages of the animals can fit at the bottom of the chamber. **b**, An adult C57BL/6 mouse with microwire bundle implantation. **c**, An implanted microwire bundle removed from the animal after recording. The arrow indicates that the skull closed around the guide cannula after 3 months of recording. **d**, Nissl staining shows that the mirowire bundle track (white arrow) reached the ventral pole of the VMH. Scale bar: 200 µm.

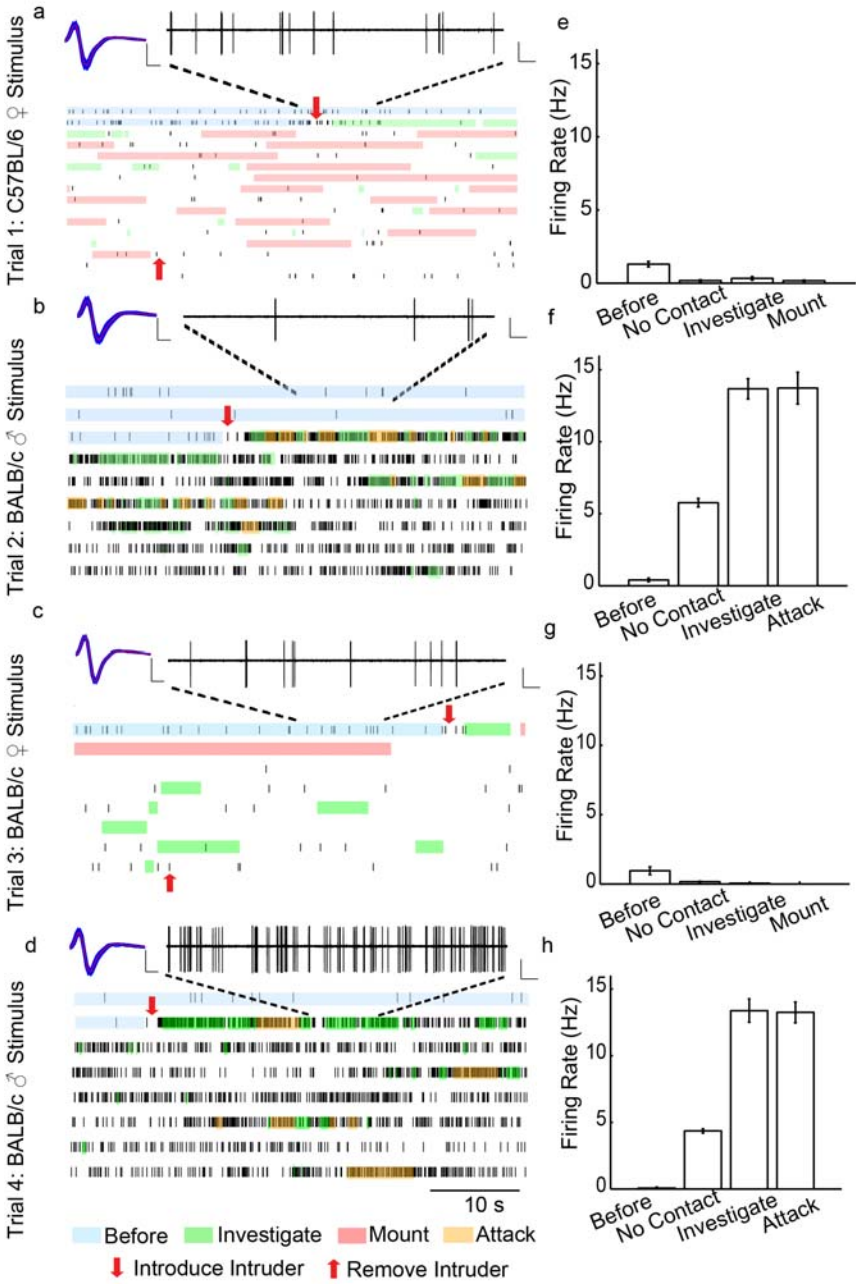

Supplementary Figure S8. Representative response patterns of a neuron in VMHvl during social behaviors

a-d, Raster plots of four continuous recording for 450-700 s of the same cell during successive exposure to test animals of the sex and strain indicated to the left. The raw recording trace expanded from the region marked by the dashed lines is illustrated at the top. Superimposed spikes are shown at the left upper corner; average spike shape is shown in red. Note that the spike shape is consistent throughout the trials. Scale bars (left): 900 μV, 200 μs. Scale bars (right): 800 μV, 1 s. The colored shading and arrows above and below the raster plots mark the behavioral episodes annotated manually. Blue: Before introduction of the stimulus animal; Green: Investigation of the stimulus animal; Red: Mounting the female; Orange: Attacking the male; Downward red arrow: Introduction of a stimulus mouse; Upward red arrow: Removal of the stimulus animal. e-h, Histograms showing the average firing rate during each behavioral episode. "Before" indicates prior to introducing the stimulus animal; "No contact" indicates time periods during which the intruder and the resident had no physical contact. Error bars: ± SEM.

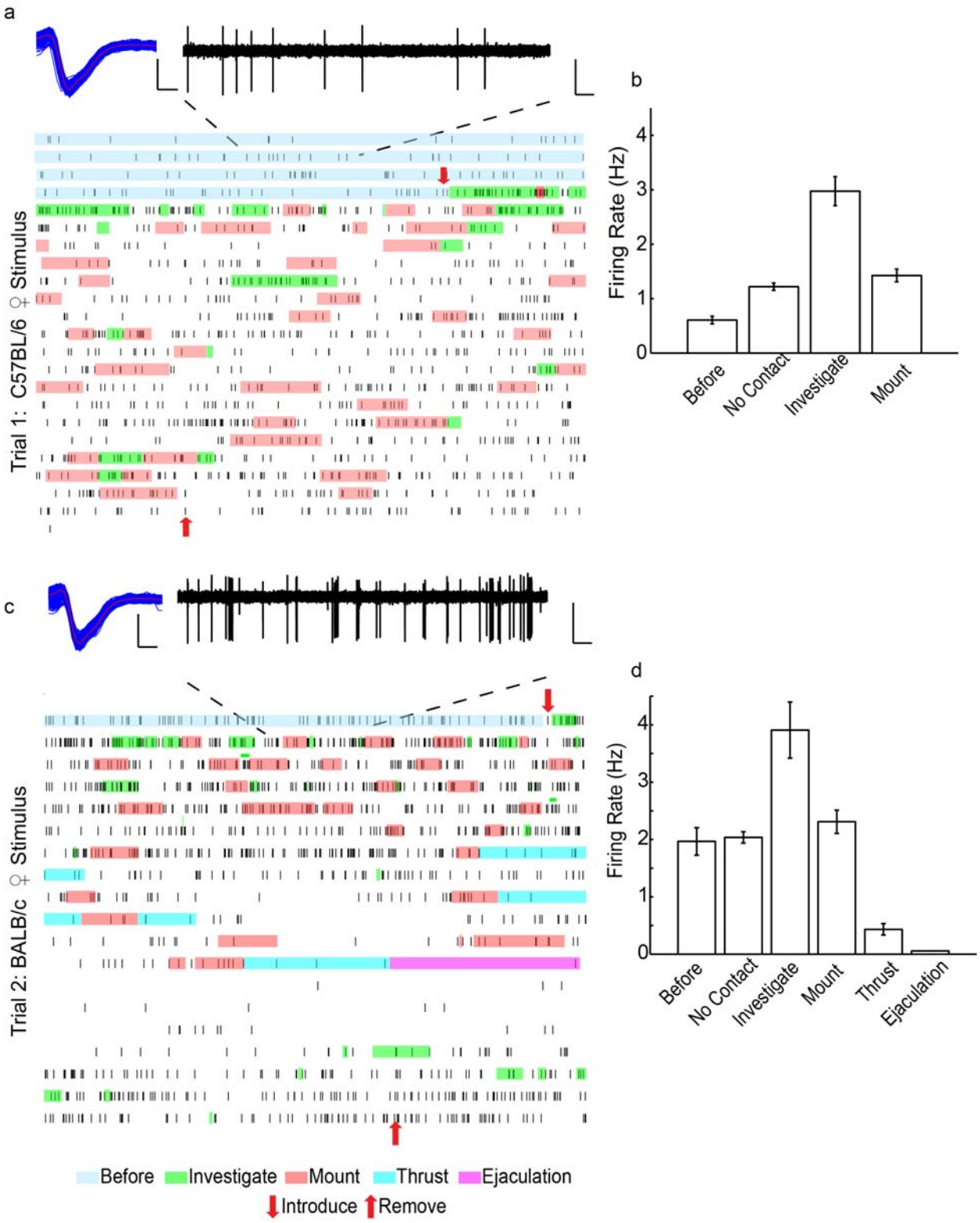

Supplementary Figure S9. Sample raster plots of VMHvl cell responses to females during mating
An example of a VMHvl cell response during social behaviors with C57BL/6 female (a, b) and BALB/c female (c, d) . Raster plots in (a) and (c) last 1100 and 950 s, respectively. Annotation conventions follow Supplementary Figure S8. Vertical scale bars: 200 μV; Horizontal scale bars on the left: 200 μs; Horizontal scale bars on the right: 1 s. Error bars: ± SEM.

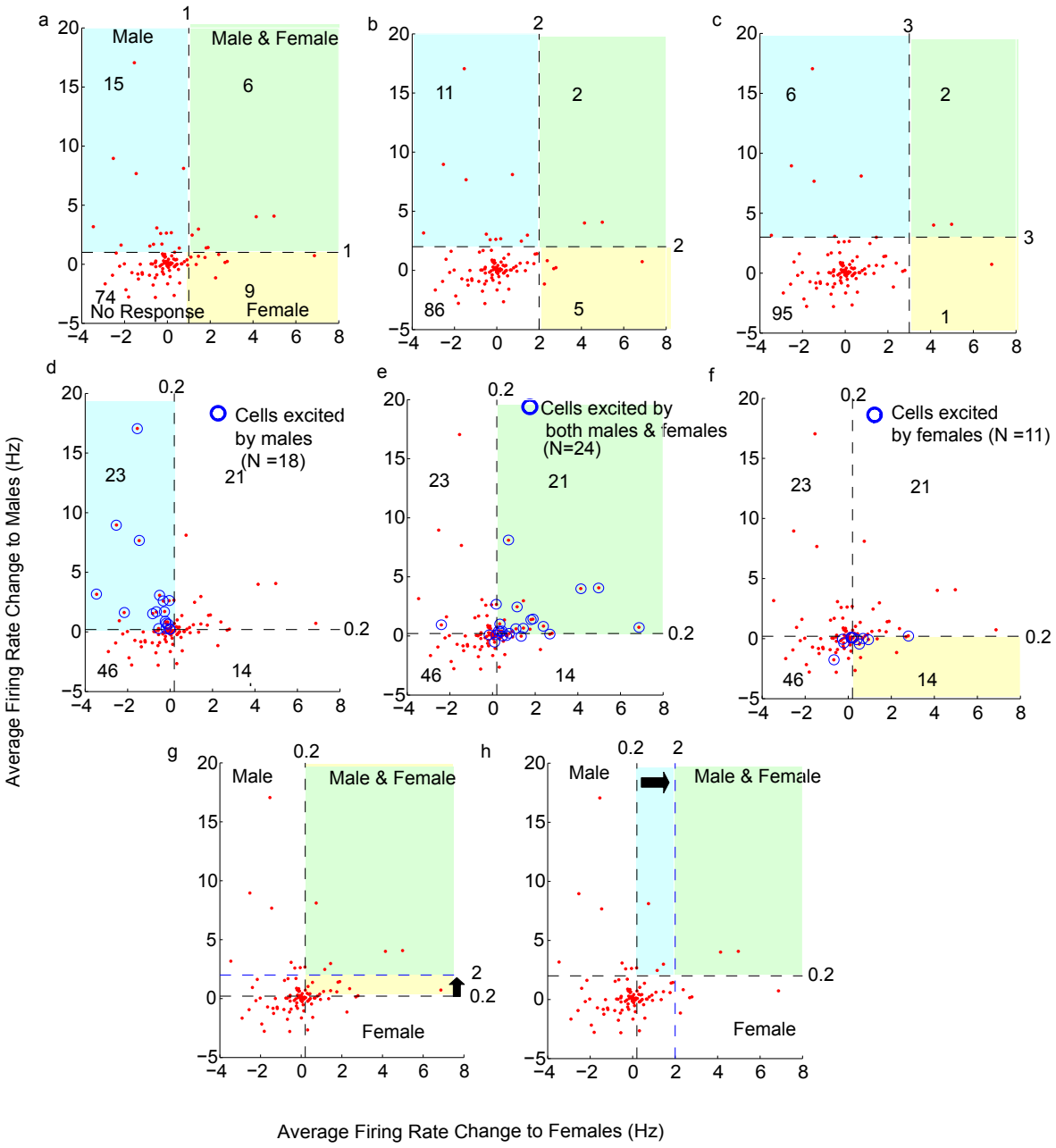

Supplementary Figure S10. Average firing rate changes during male-male and male-female social behaviors
Scatter plots of average firing rate change (an index of cumulative cell responses during the period of the social encounter) to females (x axis) and males (y axis). a-c show how different sensitivity thresholds (1 Hz, 2 Hz and 3 Hz; dashed lines), can result in a different distribution of cell response specificities. The number of units falling into each quadrant is indicated; these quadrants correspond to one of four response profiles (excited by males only, females only, both males & females and no response). d-f, Data points exhibiting a statistically significant change in firing rate during at least one behavioral episode within each social encounter are encircled in blue. A 0.2 Hz threshold (dashed line) maximizes the number of statistically significant cells above the cutoff in each of the respective quadrants, while minimizing the number of statistically non-significant cells (red points without blue circle). g, shows the reduction in the number of male-responsive cells as the detection threshold is increased upward; this causes cells in the 3rd quadrant (excited by males and females) to shift into the 4th quadrant (excited only by females). h, shows the reduction in the number of female-responsive cells as the detection threshold is increased rightward; this causes cells in the 3rd quadrant to shift into the 1st quadrant (excited only by males). Thus, increasing the threshold decreases the proportion of "double-positive" (3rd quadrant) cells. See Supplementary Footnote S1 for further details.

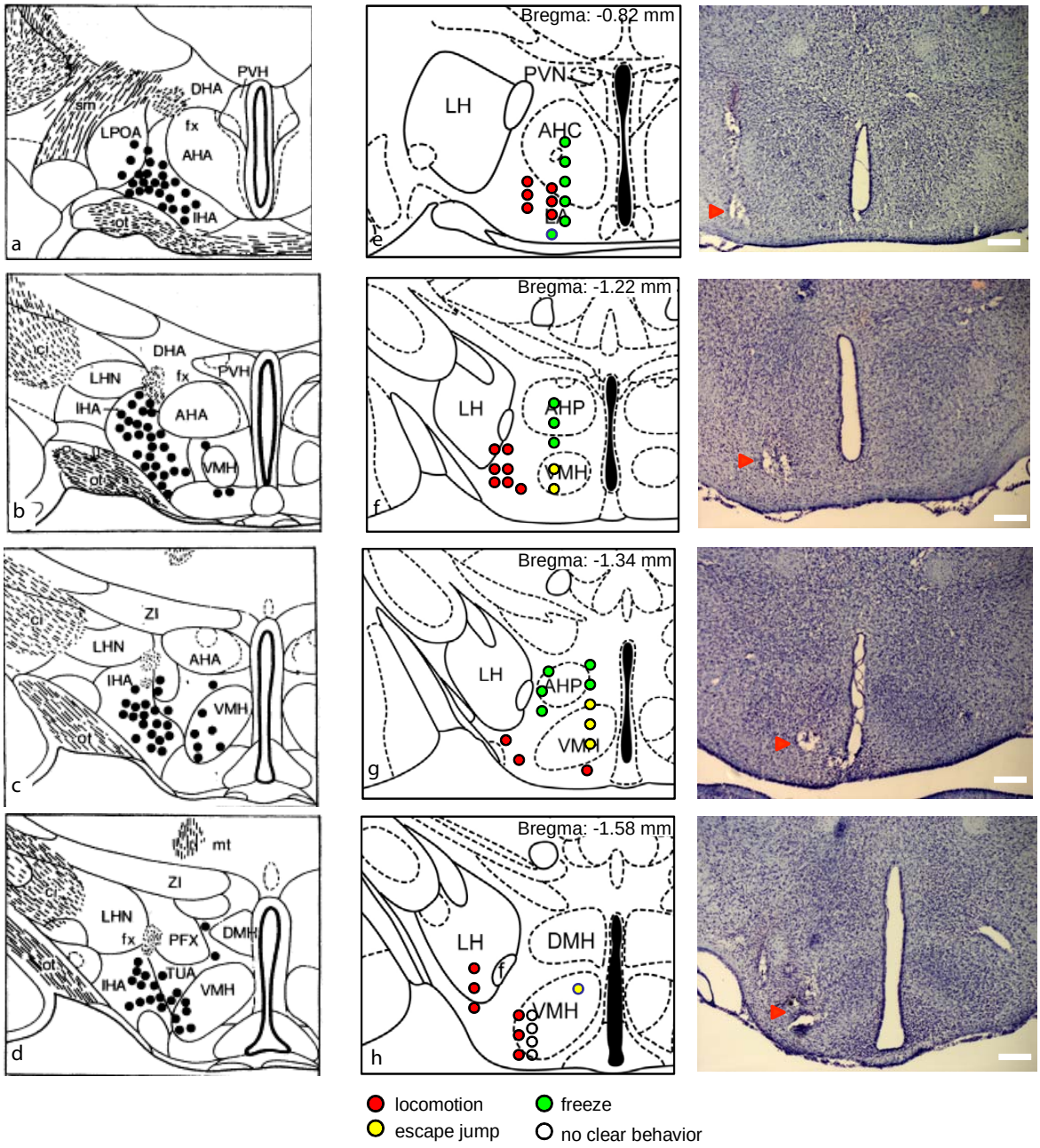

Supplementary Figure S11. Summary of the results of electrical stimulation of the HAA-homologous region in mice

a-d, Black dots mark the Hypothalamic Attack Area (HAA) in rats. Pictures were taken from Fig. 6 in Siegel A. et al. (1999)7. AHA, anterior hypothalamic area; ci, capsula interna; DHA, dorsal hypothalamic area; DMH, dorsomedial hypothalamic nucleus; fx, fornix; LHN, lateral hypothalamic nucleus; LPOA, lateral preoptic area; mt, mammillothalamic tract; ot, optic tract; PFX, perifornical nucleus; PVH, paraventricular hypothalamic nucleus; sm, stria medullaris; VMH, ventromedial hypothalamic nucleus; ZI, zona incerta. e-h, Colored dots indicate the stimulation sites in this current study mapped onto the same maps shown in (a-d). No attack could be elicited in mice from the area corresponding to the rat HAA by electrical stimulation. Colors represent the type of behaviors elicited from the site during stimulation. Red dots: locomotion, quick movement from one side of the cage to the other; Green dots: defense, maintain the same posture with little movement. Yellow dots: escape jump, aimed jump trying to escape from the cage. white dots: No clear change in behavior. i-l, Nissl staining from four representative animals. Red arrowheads indicate the tip of the bipolar stimulation electrodes. The sections in (i-l) and the illustrations in (e-h) are at the same Bregma levels. Scale bars: 250µm.

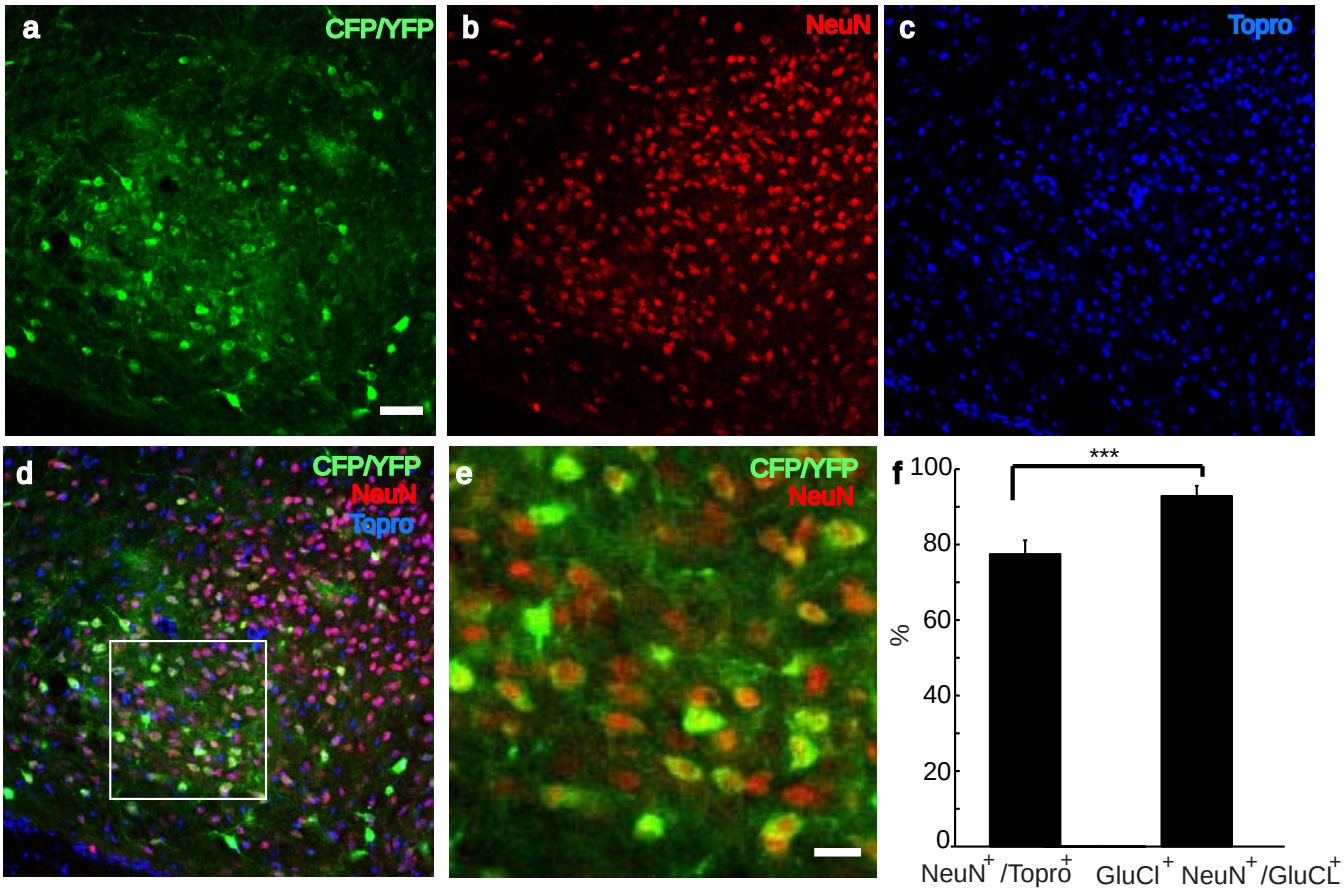

Supplementary Figure S12: AAV2-GluCL infect mainly neurons

a-e, double immunostaining of CFP/YFP (green, GluCl infected cells) and NeuN (red, neurons) in the VMHvl. Blue: Topro nuclear staining. **e** shows the enlarged area marked in (**d**). **f**, Histograms show the percentage of cells in the VMHvl as neurons (left) and the percentage of GluCl infected cells as neurons (right) (***, $p<0.001$, t-test). Error bars: ±SEM.

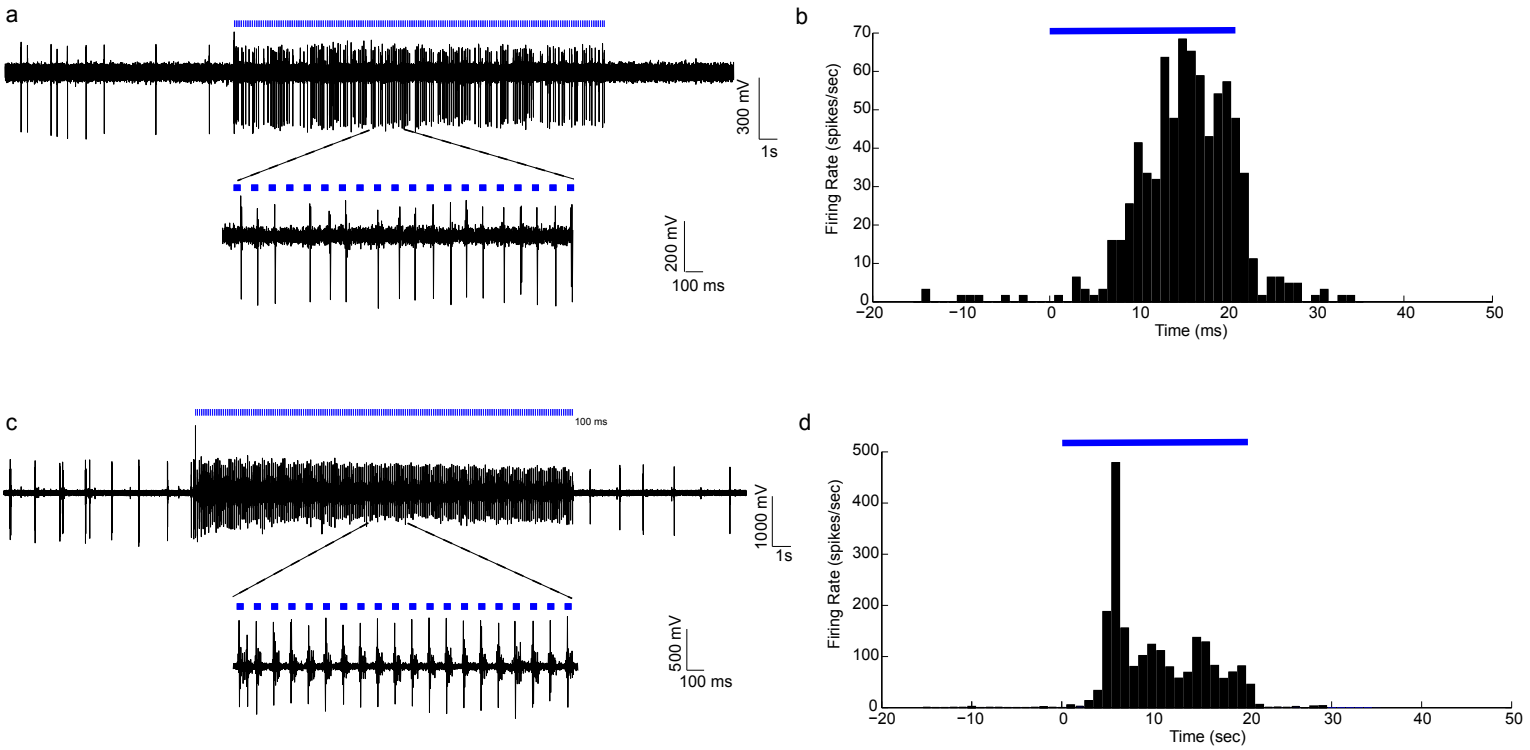

Supplementary Figure S13. Single unit recording of light induced responses of ChR2 expressing cells

a, Raw recording traces of cell activities during 1mW blue light presentation (shown as blue ticks on top of the recording trace). The dashed line marks a 1sec recording period shown in an expanded view below. Vertical and horizontal bars in (**a**): 300mV and 1s. Vertical and horizontal bars for the expanded trace: 200mV and 100ms. **b,** Histogram shows the increased firing rate during light presentation (blue bar). **c** and **d,** show a second example of a cell responses during light stimulation. Scale bars in (**c**): 1000mV and 1s. Scale bars in the expanded view in (**c**): 500mW and 100ms.

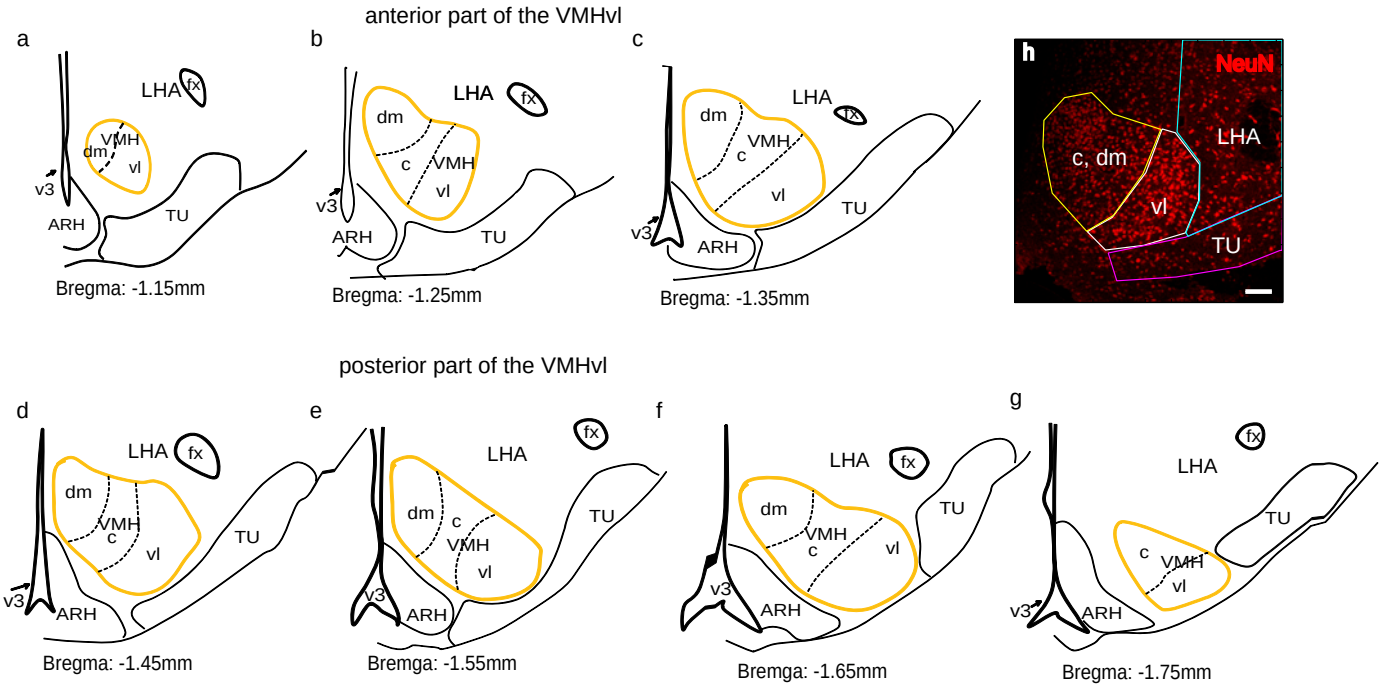

Supplementary Figure S14. Schematics indicating the reference atlas plates used for histological analysis in the activation and inactivation experiments

a-g, Anatomical structures are based on the Allen Brain Reference Atlas (www.brain-map.org). fx: Fornix; ARH: Arcuate nucleus; v3: Third ventricle; TU: Tuberal nucleus. (**a-c**) is regarded as the anterior portion of the VMHvl in this study, while (**d-g**) is the posterior portion. **h**, A representative NeuN staining picture with polygons to mark the VMHvl, VMHdm+c, TU and LHA regions for cell counting analysis. Sale bar: 100μm.

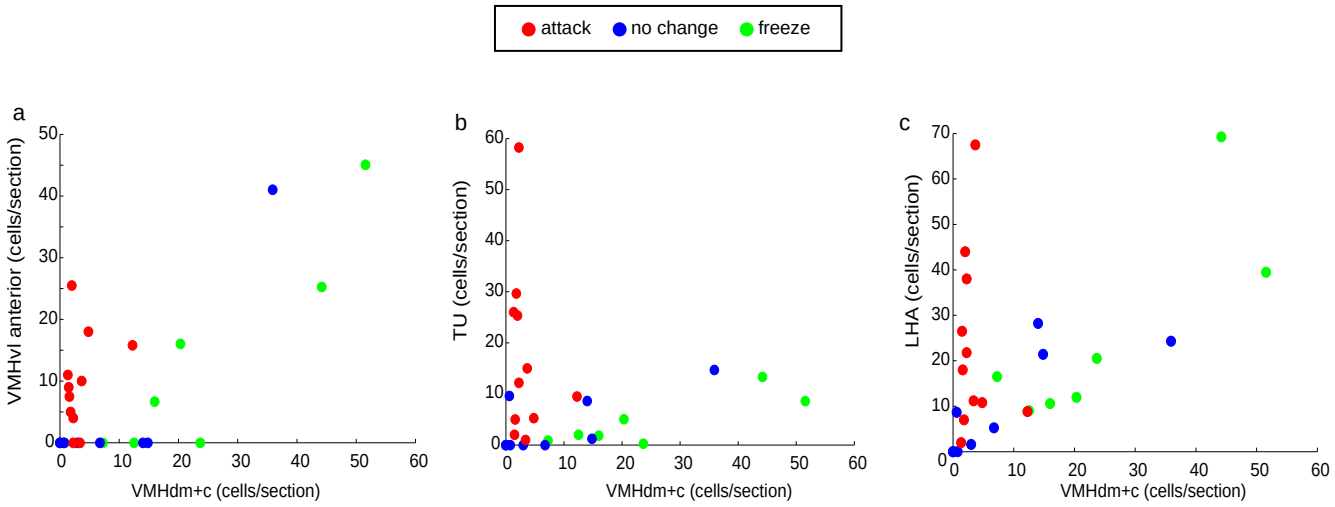

Supplementary Figure S15. No correlation between the level of ChR2 expression in surrounding regions of VMHvl posterior part and light induced behaviors

Distribution of infected cells in each animal, plotted as cells per section in VMHvl anterior part (**a**), TU (**b**) and LHA (**c**) vs. cells per section in the (VMHdm+VMHc) region. Color code indicates whether illumination induced freeze/flight (green), attack (red) or no change in behavior (blue). Attack is not correlated with the ChR2 expression in the VMHvl anterior part, TU and LHA as animals with both low and high ChR2 expression levels can be induced to attack.

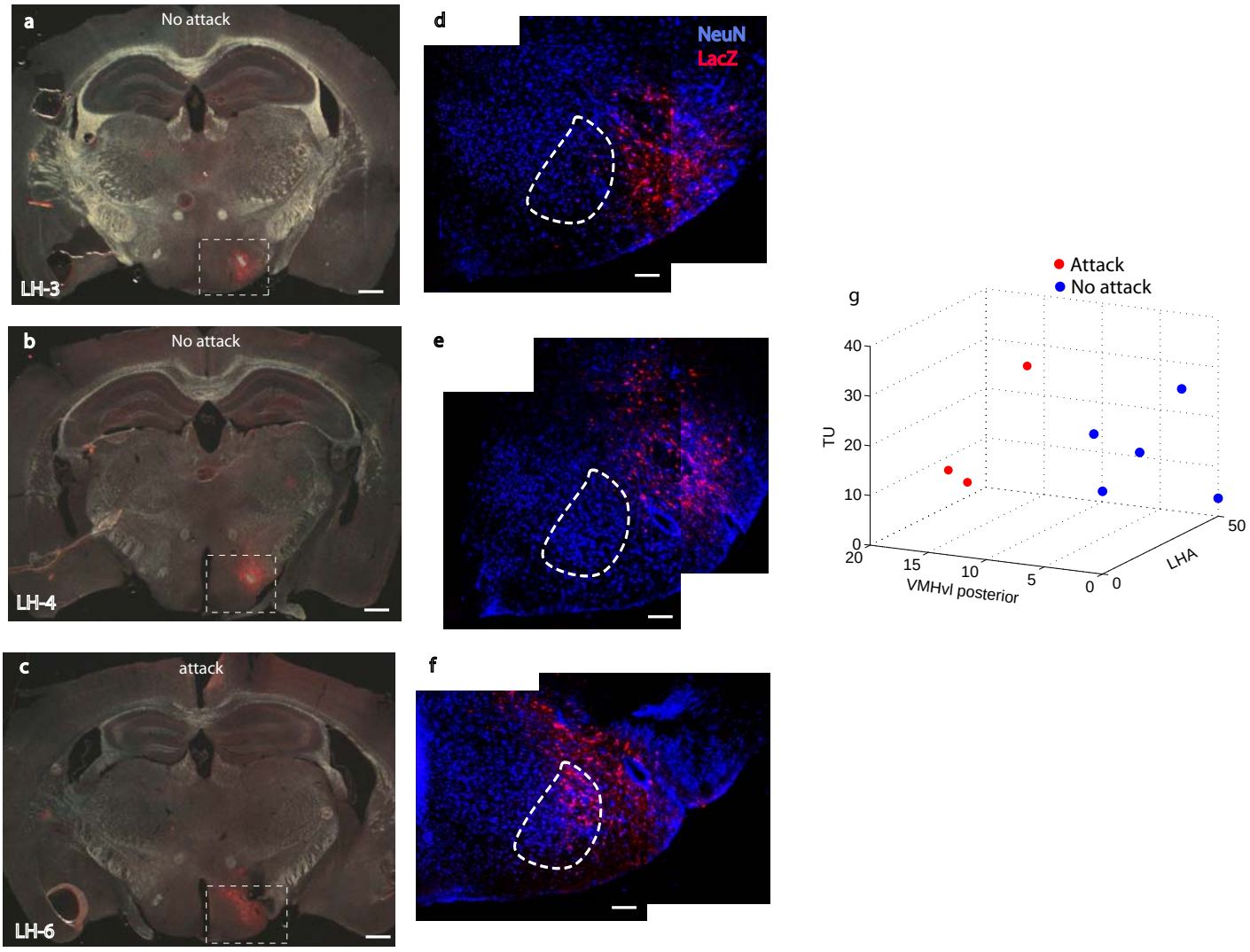

Supplementary Figure S16. Activation of VMHvl but not its surrounding regions is critical to induce attack in mice

a-c , An overview of a coronal section with anti-LacZ staining (red) from mice infected with AAV2-ChR2 and AAV2-LacZ. Attack was induced in LH-6 (**c**), but not in LH-3 (**a**) or LH-4 (**b**). Scale bars: 500μm. **d-f**, show the double immuno staining of NeuN (blue) and LacZ (red) in areas enlarged from (**a-c**). In (**d**) and (**e**), viral infection is confined to regions lateral to VMHvl while in (**f**) the virus spreads into the VMHvl (marked by dashed white outline). Scale bars: 100μm. **g**, 3D scatter plots show the infection level (No. of cells/section) in VMHvl posterior part, lateral hypothalamus (LHA) and tuberal nucleus (TU) in the 8 animals tested. Animals that were induced to attack (red) have higher infection in the VMHvl posterior part. Animals with infections only in the TU and LHA regions didn't attack (blue) during light stimulation.

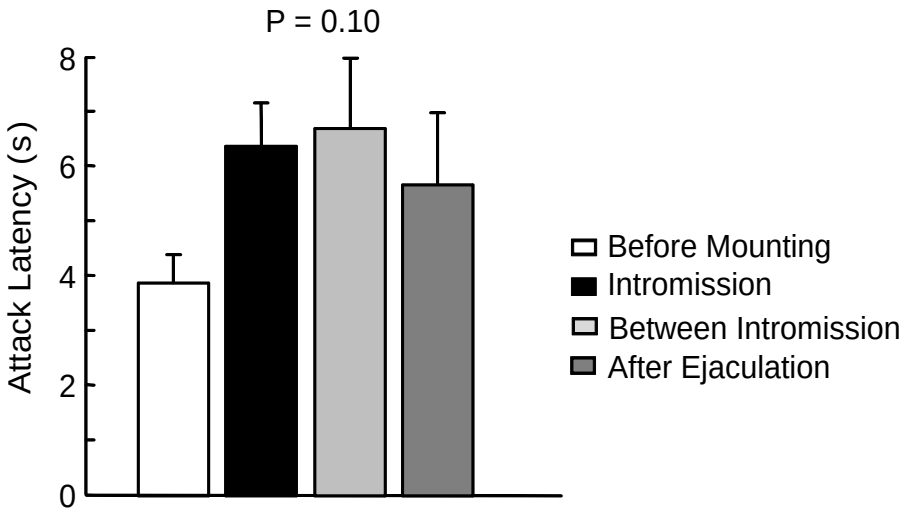

Supplementary Figure S17. Attack latency upon optogenetic activation of VMHvl during various stages of mating with a female

The attack latency following light stimulation during intromission (black bar), between intromission (light gray bar) and after ejaculation (dark gray bar) has a tendency to be longer than the attack latency before mounting (white bar) (p = 0.10 by one-way ANOVA).

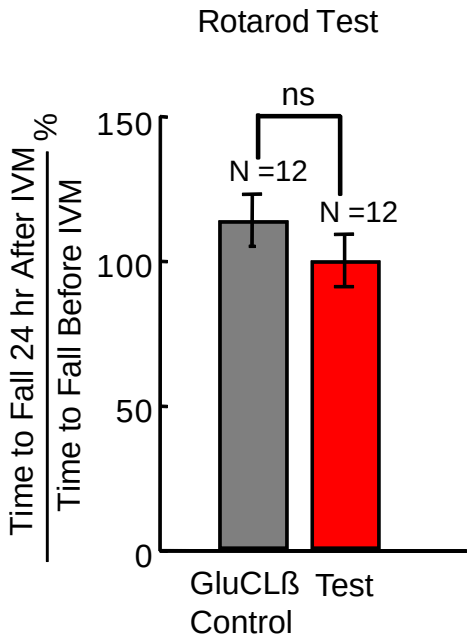

Supplementary Figure S18. No change in motor coordination after viral inactivation of the VMHvl

Both the test group (n = 12; red bar) and the GluClβ injected control group (n = 12; gray bar) showed no change in the amount of time spent on the rotarod before and 24hr after ivermectin injection.

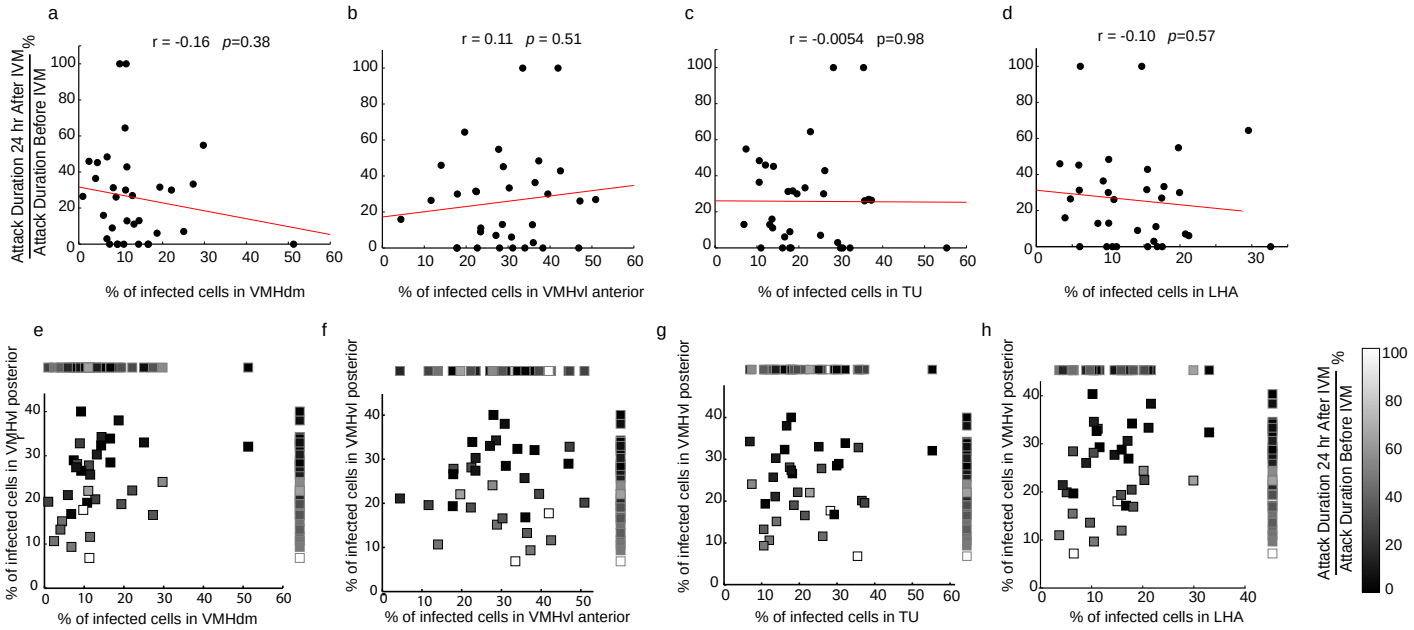

Supplementary Figure S19. No correlation between infection level in various regions surrounding the VMHvl posterior part and aggression level change

a-d. Percentage of infected cells in VMHdm (**a**), VMHvl anterior portion (Bregma -1.15 — -1.4mm)(**b**), TU (**c**) and LHA (**d**) plotted against the extent of aggression suppression after IVM injection. The infection level in those areas are not significantly correlated with the aggression suppression. e-h, Gray scale coded scatter plots using infection levels in two regions as x and y values and the level of aggression change as marker face color. Each marker represents one animal. The % of infected cells in VMHvl posterior (y axis) is a strong predictor of the aggression suppression (that is, the remaining aggression level decreases along the ordinate), whereas the infection level in other regions are poor predicators of any aggression decrease (that is, both black and white colors are represented along the full length of the abscissa). The top and right side of each plot shows all the markers projected onto the x and y axis to reveal the behavioral variation along that axis. A calibration bar representing the percentage of remaining aggression level (The ratio between Attack Duration 24hr after IVM and Attack Duration before IVMH x100%) is shown on the far right.

SUPPLEMENTARY METHODS

Fos catFISH

Digoxigenin- and 2,4-Dinitrophenol (DNP)-labeled *fos* cRNA and *fos* intronic probes were detected using horseradish peroxidase-conjugated antibodies on 20 µm fresh frozen sections. The signals were amplified using Biotin and DNP conjugated tyramide (PerkinElmer) and subsequently visualized using Alexa 488-conjugated streptavidin and Alexa 555-conjugated DNP antibody (Invitrogen). Topro was used for nuclear counterstaining (1:2000, Invitrogen). The *fos* intronic probe contains the entire first intron of the *fos* gene. The *vglut2* probe has the same sequence as in the Allan Brain Atlas database.

Confocal microscopy and cell counting

Details of the imaging procedure have been described previously[1]. In brief, z-section image series (~0.7 µm optical thickness) of the lateral septum ventral part (LSv), nucleus accumbens (AcbC), paraventricular nucleus (PVN), dorsal medial hypothalamic nucleus (DMH), medial preoptic nucleus (MPN), ventrolateral part of ventromedial hypothalamic nucleus (VMHvl), tuberal region (TU), premammillary nucleus ventral part (PMv), bed nucleus of the stria terminalis posterior part (BNSTp), supraoptic nucleus (SON), substantia innominata (SI), medial amygdala anterior part (MEAa), medial amygdala posterior dorsal part (MEApd), medial amygdala posterior ventral part (MEApv), cortical amygdala posterior lateral part (COApl),cortical amygdala posterior medial part (COApm), periaqueductal gray dorsal part (dPAG), periaqueductal gray ventral part (vPAG), periaqueductal gray lateral part (lPAG), subparafascicular nucleus thalamus, parvicellular part (SPFp), paraventricular nucleus thalamus (PVT) and piriform cortex (PIR) of each animal were collected with a 40x objective to quantify the number of *c-fos*$^{+}$ cells, and determine the subcellular location of the *c-fos* mRNA. The anatomical structure was assigned mainly based on the Topro counter staining and sometimes by reference to Nissl staining on an adjacent section. Images were taken only from regions where the structure assignment could be made with confidence. During the image acquisition and subsequent counting, the slides were coded so that the experimenter was blind to the actual behavioral condition.

Immunohistochemistry

The following primary antibodies were used: Goat anti-c-Fos (1:300; Santa Cruz Biotechnology), rabbit anti-GFP (1:300, Invitrogen), chicken anti-LacZ (1:500, Abcam), mouse anti-NeuN (1:500, Millipore). The fluorophore-conjugated secondary antisera used were: Dylight 549 Donkey anti-Chicken (1:300, Jackson ImmunoResearch), Cy3 donkey anti-goat (1:300, Jackson ImmunoResearch), Alexa 488 donkey anti-rabbit (1:300, Invitrogen), Cy5 donkey anti-mouse (1:300, Jackson ImmunoResearch). NeuroTrace 660 was used for fluorescent Nissl staining (1:100, Invitrogen).

Electrical stimulation

Animals were stereotactically implanted with tungsten or stainless steel bipolar stimulating electrodes (Microprobes) attached to a custom made movable driver. The initial implantation depth was 5.3mm. After the animal recovered from the surgery fully (1 week to 10 days) and on days of testing, a flexible cable was attached to the microdrive and connected to a torqueless passive commutator (Dragonfly). During testing, the animal was allowed to stay in its home cage and interact with the stimulus animals freely. Female, castrated male or male mice were introduced into the test arena while biphasic stimulation current (0.2ms at 20Hz) was passed through the bipolar electrodes for 10 seconds every one to two minutes. Stimulation current was initially 10μA and was increased in incremental steps of 20μA until an obvious behavioral change was observed, or until the current reached 200μA. Typical thresholds for a behavioral change were between 30-90μA. A behavioral change was scored as positive if it could be repeatedly elicited at least 3 times. The same behavior could often be elicited in multiple test sessions over several days. After testing the initial implantation site one to three times (depending on the behavioral change), the electrodes were moved downwards by 140μm to reach the next test location, to a maximum depth of 6.0mm. After the completion of behavioral testing, brains were harvested for histological analysis.

Optotrode recording

Animals were stereotactically injected into the VMHvl region with a mixture of 240nl Cre-inducible AAV2 [EF1α::ChR2-EYFP], AAV2 [CMV::CRE], AAV2 [CMV::LacZ] at 4:2:1 volume ratio to reach a similar final titer ($8x10^{11}$ pfu/mL) as described above. Three weeks later, extracellular recording was obtained from the injection site using the same stereotactic coordinates, while the animals were under anesthesia. Recording and light stimulation was achieved using tungsten electrodes (1.5MΩ, microprobes) bundled with a 200 µm multimode optical fiber (Thorlabs) as described before[2]. Light was delivered at 20ms, 20Hz at intensities from 1mW to 4mW at the tip of the fiber. After recording was completed, brains were harvested for histological analysis to confirm that the center of the injection site was in the VMHvl.

SUPPLEMENTARY FOOTNOTES

Supplementary Footnote SF1. Our fos catFISH data suggested that most cells in VMHvl are specifically activated during encounters with either males or females, with only 20-30% of the cells activated during both types of encounters. In contrast, our electrophysiological analysis indicated that ~ 47% (25/53) of cells are activated during encounters with both males and females. This apparent discrepancy likely reflects the greater sensitivity of electrophysiology, and the fact that the electrophysiological analysis identifies statistically significant changes, while *c-fos* induction identifies large magnitude changes. The statistical analysis that we used to identify cells responsive to a given stimulus assigns a cell as "responsive" (excited or inhibited) if it exhibited a statistically significant change in its firing rate over the period of a given behavioral episode (investigate, mount, attack, etc.), compared to the background firing rate prior to introduction of the stimulus animal (see Supplementary Methods). By contrast, the fos catFISH analysis reflects the integrated activity of a neuron over a time period that spans the entire encounter with the stimulus animal (typically 5 min). Furthermore, the electrophysiological analysis is independent of the magnitude of the change in response; thus an increase of small magnitude could be scored as a significant change, while a large magnitude increase might not reach significance. In contrast, *fos* induction is proportional to the level of activity.

In order to better correlate our electrophysiological analysis with the fos catFISH analysis, we first re-analyzed our recordings by developing a continuously varying metric, rather than a binary (significant vs. not-significant) one. We calculated the mean change in firing rate for each unit, over the entire period of each encounter (Fig. 3d). This parameter is more likely to be reflected in the level of *c-fos* induction, than is the all-or-none assignment of a statistically significant change in firing rate during individual behavioral episodes (which may last only a minute or less). These values are presented as a two-dimensional scatter plot in Supplementary Figure S10. Each point on the scatter-plot is assigned its coordinates based on its average change in activity during encounters with males (y-axis), and its average change in activity during encounters with females (x-axis). It is apparent that most of the data points have relatively low x-y values (i.e., lie in the lower-left quadrant, Fig. S10a; median response to males = 0.06 Hz; median response to females = -0.01 Hz).

Next, we computationally reduced the sensitivity of this continuous variable analysis by filtering the data to exclude cells exhibiting low average firing rate changes. When only those cells that exceeded a threshold average firing rate change of 1, 2 or 3 Hz were included in the analysis (Figs. S10a-c), more cells were "single-positive" (i.e., activated above threshold by either a male or a female stimulus; Fig. S10a, blue and yellow quadrants) than were "double-positive" (activated above threshold by both stimuli; Fig. S10a, green quadrants). At 1 Hz and 2 Hz, the proportion of "double-positives" among all positive cells (above threshold) was 20% and 11.1%, respectively (Figs. S10a and b). The 2 Hz threshold, in particular, yielded a fraction of excited cells activated by both males and females remarkably similar to that measured in the fos catFISH analysis. (The reason that the proportion of double-positives decreases as the threshold is increased is that most "double-positive" cells are unequally activated by the two types of stimuli--i.e., most points do not lie along the diagonal (Fig. 3d). Thus, as the threshold is increased symmetrically along both axes, one of the x-y values for most data points will drop below threshold before the other; hence data points will tend to shift from the "double-positive" quadrant into one or the other of the single-positive quadrants. Increasing the cutoff for activation by a female will shift more cells into the "male-only" quadrant (Fig. S10h), while increasing the cutoff for activation by a male will shift more cells into the "female-only" quadrant (Fig. S10g). This analysis indicates that when the electrophysiological data are

analyzed using a continuous rather than a binary metric, and the sensitivity of the method is decreased to exclude cells with small changes in firing rates, the conclusions are quantitatively concordant with the results of the catFISH analysis: Most of the cells are activated either by a male or a female intruder, but not by both, while only a small proportion (10-20%) are activated by both stimuli.

We also investigated the relationship between the two criteria used to parse our recordings: 1) whether the cumulative firing rate change for each cell across the entire social encounter was above a certain threshold; and 2) whether the cells exhibited a statistically significant change in firing rate within any one behavioral episode during the encounter. Data points that met the second criterion are encircled in blue in the scatter-plots illustrated in Figs. S10d-f. Most of the cells that exhibited changes in firing rate > 1 Hz in response to males, or both males and females, also exhibited statistically significant changes. (In the case of females, most of the significant cells exhibited average firing rate changes < 1 Hz; Fig. S10f). Thus, the cells that are more likely to be detected by c-fos analysis are also the cells that show statistically significant increases in firing rate. Finally, we asked whether there was a threshold firing rate that maximized the number of statistically significant (red with blue circle) points above the cutoff, while minimizing the number of statistically not significant points above the cutoff (red dots without circle), for all three categories of responses (male-specific, female-specific, male+female). Such a threshold value was found at 0.2 Hz (Figs. S10d-f). Using this threshold, the fraction of statistically significant "double-positive" cells (i.e., cells responding to both males and females) is higher (36%; Fig. S10e) than obtained when the threshold is set at 2 Hz (11%). Thus, when a cutoff value of ~2 Hz is used, which captures the most strongly activated, but not all the statistically significant, cells, the proportion of VMHvl cells activated by both males and females is more similar to that observed using the fos catFISH analysis, than when a threshold cutoff is used that captures the maximum number of statistically significant cells (0.2 Hz). Consistent with this ~10-fold difference, over 40% of all units showed a statistically significant change in firing rate during exposure to a male (Fig. 3c), while only ~4% of all cells in VMHvl expressed nuclear *c-fos* transcripts following a 5-minute exposure to a male intruder (Fig. S5, VMHvl).

This analysis reveals that a difference in sensitivity can explain why our electrophysiological analysis detects a higher proportion of cells activated by both males and females in VMH, than is detected by the fos catFISH analysis. Importantly, most of the "double positive" cells detected by electrophysiology exhibited relatively small (< 2 Hz) average changes in firing rate during the behavioral encounters. Thus, among cells showing large and statistically significant increases in firing rate, the majority (80-90%) responded either to males or females, but not to both. Notably, a higher proportion (1.6 to 3-fold) of VMHvl cells were activated only by males, than only by females, irrespective of whether average firing rate change (> 1 Hz), or statistical significance was used as a metric, consistent with the fos catFISH data (Fig. S5, VMHvl).

Supplementary Footnote SF2. To activate VMHvl artificially, we initially used bipolar electrodes to stimulate the VMHvl region in awake behaving mice. In rats and cats, this method was successfully employed to elicit attack in the medial hypothalamus[3]. However, no attack was induced among the 40 mice we tested even though many animals had electrodes placed in VMHvl or adjacent regions (Fig. S11). Instead of attacking, a typical behavioral change upon such electrical stimulation was freezing or flight, even when the animal was engaged in intensive fighting prior to stimulation. Since electric current also activates fibers of passage, it is likely to activate axons from the nearby VMHdm, which is a critical relay in defense pathways[4], and this may override any activation of the VMHvl. In rats, it was reported that depending on the context both flight and fight can sometimes be induced from the same site, indicating the close proximity of regions mediating defense and aggression[5]. Due to the significantly reduced size of the mouse brain compared to the rat brain, electrical stimulation may not be sufficient to resolve the defensive area[6] from the aggression area[7].

Supplementary Footnote SF3. To confirm that AAV2 vectors mainly infect neurons as shown previously[8-9], we performed triple staining with GluCl, NeuN and Topro nuclear staining in AAV2-GluCl injected animals. Approximately 77% of all VMHvl cells are neurons while 93% GluCl positive cells in the VMHvl are neurons, indicating that AAV2 indeed preferentially infect neurons (Fig. S12). To confirm that the AAV2 vector does not retrogradely infect axons innervating or passing through VMHvl, we examined MEA and BNST, two major input regions

to VMHvl. No virally infected cells were found by either intrinsic (native) CYP/YFP fluorescence, or by immunostaining. Coarse investigation of the brain regions between Bregma 0.8 mm to -5.5 mm at 10x magnification revealed no infection at locations other than the intended injected site.

Supplementary Footnote SF4. To provide a more quantitative approach to analyzing the ChR2 activation experiments, as the reviewer requested, we have constructed a multinomial logistic regression model to analyze the relationship between the level of infection in various areas and the behavioral outcome. Multinomial logistic regression is a regression model used when the dependent variable (the behavioral outcome in this case) is a set of categories that cannot be ordered in any meaningful way. This is true in the present case because the outcomes are represented by binary categories: defense (freezing and/or flight); attack; no change. A simple logistic function can be defined by the formula:

$$f(z) = \frac{e^z}{e^z + 1} = \frac{1}{1 + e^{-z}} \quad \text{(Equation1)}$$

The variable z represents the exposure to a set of independent variables, while $f(z)$ represents the probability of a particular outcome, given that set of explanatory variables. z is a measure of the total contribution of all the independent variable and is usually defined as:

$$z = \beta_0 + \beta_1 x_1 + \beta_2 x_2 + \beta_3 x_3 + \cdots + \beta_k x_k, \quad \text{(Equation 2)}$$

Where β_0 is called the intercept and β_1, β_2 β_3 and so on denote the regression coefficients of independent variables x_1, x_2, x_3 respectively. The regression coefficient β describes the contribution of each variable. A positive regression coefficient means that the variable increases the probability of a given outcome, while a negative regression coefficient means that the variable decreases the probability of that outcome. A large regression coefficient means that the variable strongly influences the probability of that outcome. A near-zero regression coefficient means that the variable has little impact on the outcome. The maximum likelihood method is used to estimate the regression coefficient of the multinomial regression model through an iterative fitting process. To apply the multinomial logistic regression model, a minimum ratio between the sample size and the number of independent variables ~ 10 is recommended. Given

our sample size (N=35), therefore, such a model could support 3 variables. The Matlab function "mnrfit" was used to determine the regression coefficients of the model. The level of infection in "VMHdm+c", "VMHvl" and "LHA+TU" were used as the three explanatory variables in the model. The behavioral outcomes "defense", "attack" and "no change" were used as three dependent variables. Since multinomial logistic regression compares multiple groups through a combination of binary logistic regressions, we used the "no change" group as the reference group for the "attack" and "defense" groups. Below are the results of the analysis:

Table 1:

Model	Model fitting Criteria	Likelihood Ratio Tests		
	-2 Log likelihood	Chi-Square	df	*p* Value
Intercept Only	75.02			
Final	21.49	53.53	6	<0.0001

Table 2:

Omitted Variable	Model Fitting Criteria	Likelihood Ratio Tests		
	-2 Log Likelihood of Reduced Model	Chi-Square	df	*p* Value
VMHdm	64.10	42.61	2	<0.0001
VMHvl	53.75	32.26	2	<0.0001
TU_LHA	23.82	2.33	2	0.311

Table 3:

Attack	Regression coefficient	Std. Error	*p* value
Intercept	-5.467	2.961	0.068
VMHdm	-1.376	0.466	0.003**
VMHvl	0.898	0.286	0.002**
LHA +TU	-0.037	0.054	0.500

Table 4:

Defense	Regression coefficient	Std. Error	*p* value
Intercept	-0.992	0.906	0.108
VMHdm	0.514	0.244	0.035*
VMHvl	-0.355	0.228	0.120
LHA+TU	-0.053	0.065	0.418

* <0.05 ** <0.01

Table 1 shows the test for goodness-of-fit. A low p value indicates that the model is a significantly improved fit compared to null hypothesis ($\beta_1 = \beta_2 = \beta_3 = 0$). Table 2 shows the results for Likelihood Ratio tests to compare the final model with different reduced models. The reduced models are formulated by omitting an independent variable from the final model. A low p value for a given variable (site of infection) indicates that this variable made a significant difference for the goodness-of-fit if omitted from the original model. In such cases, the variable contributes significantly to explaining the dependent variable (behavioral outcome). The results in Table 2 indicate that the infection rates in VMHvl and VMHdm are significantly related to the behavioral outcome, while the infection rate in LU+LHA is not.

Tables 3 and 4 show how critical the independent variables are in explaining the different behavioral outcomes (Attack vs. No Change; Defense vs. No Change). The Standard Error in the second column with values < 2 (not including the intercept) suggests that the method produced a set of reasonable fittings. The regression coefficients suggest that infection in VMHdm contributes negatively to the likelihood of an attack outcome, while infection in VMHvl contributes positively. The p values in the third column represent the probability that one would have observed the current behavioral outcome if the coefficients of the independent variables were equal to 0 (null hypothesis). If $p < 0.05$, the corresponding independent variable (infection level in that brain region) exerts a significant effect on the particular behavioral outcome. Therefore, the infection level in "VMHdm" and "VMHvl" is significantly related to the attack outcome, while the infection in the LHA+TU is not. VMHdm is significantly related to the "defense" behavior while the VMHvl and LHA+TU infection level is likely to be uncritical (although the coefficient for VMHvl is negative for the freezing outcome, the opposite of its sign for attack).

SUPPLEMENTARY MOVIE LEGENDS

Supplementary Movie S1. Response of a neuron recorded from a C57BL/6 male during investigation and attack of a BALB/c male. Sound, playback of spiking activity. Note the increased cell activity before the physical contact occurs.

Supplementary Movie S2. Response of the same neuron shown in Supplementary Movie 1 during investigation and mounting of a BALB/c female. Note the sustained decrease in cell activity in the presence of the female.

Supplementary Movie S3. Attack towards a BALB/c female is induced by light stimulation of a C57BL/6 male mouse in the VMHvl region. The LED light on the left corner indicates the time period during which 1 mW/mm^2 pulsing blue light (20 ms, 20 Hz) is delivered through the optic fiber attached to the animal. The fiber is covered with black paint to prevent the animal from being disturbed by the light.

Supplementary Movie S4. Attack towards a glove is induced by stimulating VMHvl in a C57BL/6 male mouse.

SUPPLEMENTARY REFERENCES

1 Guzowski, J. F., McNaughton, B. L., Barnes, C. A. & Worley, P. F. Environment-specific expression of the immediate-early gene Arc in hippocampal neuronal ensembles. *Nature neuroscience* **2**, 1120-1124 (1999).

2 Gradinaru, V., Mogri, M., Thompson, K. R., Henderson, J. M. & Deisseroth, K. Optical deconstruction of parkinsonian neural circuitry. *Science* **324**, 354-359, doi:1167093 [pii]10.1126/science.1167093 (2009).

3 Siegel, A., Roeling, T. A., Gregg, T. R. & Kruk, M. R. Neuropharmacology of brain-stimulation-evoked aggression. *Neuroscience and biobehavioral reviews* **23**, 359-389 (1999).

4 Canteras, N. S. The medial hypothalamic defensive system: hodological organization and functional implications. *Pharmacol Biochem Behav* **71**, 481-491 (2002).

5 Kruk, M. R. Ethology and pharmacology of hypothalamic aggression in the rat. *Neuroscience and biobehavioral reviews* **15**, 527-538 (1991).

6 Lammers, J. H., Kruk, M. R., Meelis, W. & van der Poel, A. M. Hypothalamic substrates for brain stimulation-induced patterns of locomotion and escape jumps in the rat. *Brain research* **449**, 294-310 (1988).

7 Lammers, J. H., Kruk, M. R., Meelis, W. & van der Poel, A. M. Hypothalamic substrates for brain stimulation-induced attack, teeth-chattering and social grooming in the rat. *Brain research* **449**, 311-327 (1988).

8 Lerchner, W. *et al.* Reversible silencing of neuronal excitability in behaving mice by a genetically targeted, ivermectin-gated Cl- channel. *Neuron* **54**, 35-49, doi:S0896-6273(07)00170-5 [pii]10.1016/j.neuron.2007.02.030 (2007).

9 Taymans, J. M. *et al.* Comparative analysis of adeno-associated viral vector serotypes 1, 2, 5, 7, and 8 in mouse brain. *Hum Gene Ther* **18**, 195-206, doi:10.1089/hum.2006.178 (2007).